Separation of cloud-affected data for PREDE sky radiometer data analyses and then study of aerosol climatology in an urban atmosphere of Chiba, Japan

Pradeep Khatri[1] and Tamio Takamura[2]
[1]CEReS, Chiba University, Chiba, Japan, Email: pradeep.nep@gmail.com
[2]CEReS, Chiba University, Chiba, Japan, Email: takamura@faculty.chiba-u.jp

Abstract

This paper firstly describes an algorithm to screen cloud-affected data for sky radiometer data analyses. The proposed algorithm is observed to screen cloud-affected more effectively in comparison to other algorithms. Secondly, aerosol climatologies in an urban atmosphere of Chiba studied by using cloud-screened data are presented. Aerosols in an urban atmosphere of Chiba are observed to show distinct seasonal variations in magnitudes and diurnal cycles of optical properties as well as magnitudes of aerosol radiative forcing. The study suggests the influence of complicated air masses in the spring season, whereas aerosols existing in the autumn season are suggested to be more capable to trap energy in the atmosphere by creating comparatively larger radiative forcing efficiency difference at that top of the atmosphere and the surface.

1.Introduction

Though aerosols are known to play an important role on atmospheric heat budget, their effects on climate change are still subject of debate. This is due to the uncertainties in aerosol optical properties and spatial distributions of aerosols. Therefore, both the quality check of data and collection of information regarding aerosol effects on atmospheric heat budget in different regions of climatic significance are important.

The continuous collection of data in SKYNET network by various instruments, including PREDE sky radiometer, are very useful for expanding our knowledge regarding aerosol effects of climate change, however, one of the challenges for using PREDE sky radiometer data is to separate clear sky and cloudy sky periods. Additionally, as several major field campaigns were mainly held over the ocean or costal regions, data of urban atmospheres are relative sparse. In view of those recognitions, this paper focuses on two important topics: (i) Development of a cloud screening algorithm for PREDE sky radiometer data analyses and (ii) study of aerosol optical properties and direct radiative forcing in an urban atmosphere of Chiba, Japan using data collected by PREDE sky radiometer.

2. Development of a cloud-screening algorithm

A detailed description of a cloud-screening algorithm is reported in a separate publication.[1)] In brief, the algorithm consists three tests: (i) test with global irradiance data, (ii) spectral variability test, and (iii) statistical analyses test. Though the test with the global irradiance data is the most powerful test, our study shows that it has some limitations, which can sometimes cause some clear sky data to be detected as cloud-affected data. In order to cope this problem, a modified version of spectral variability algorithm[2)] is proposed. As the second test, the modified spectral variability algorithm is applied to filter clear sky data from data detected as cloud-affected by the first test. Finally, statistical analyses tests (diurnal stability test, data smoothness test, and three standard deviation criteria test) are performed to remove any outlier, if exists, from clear sky data detected by the first and second tests. It is shown that our proposed algorithm can screen cloud-affected data more effectively in comparison to other cloud screening algorithms (Table 1 of Khatri and Takamura (2008)). As an example, Figure 1 shows scatter plots of aerosol optical thickness at 500nm (τ_{500nm}) and angstrom exponent (α) before and after

cloud screenings for one year data of 2006 collected in Chiba. Approximately 77% of initial data remained after cloud screening. As shown in Figure 1(b), some data with τ_{500nm} of around 1.5 still exist. Those data are less likely to be cloud-afffected because of their high values of α. Similarly, some data with high τ_{500nm} and small α (indicated by dotted closed oval) also exist. Those data are noted to fall in the spring season. Furthermore, the present algorithm is applied to dust-loaded atmospheres by taking data collected in Dunhuang in the spring season of 2006. It is discussed that the present algorithm may screen cloud affected data effectively even in the dust loaded atmosphere. For Dunhuang data, the mean value of τ_{500nm} (α) is observed to decrease (increase) by ~0.12 (~0.073) by eliminating ~36.9% of initial data after an application of cloud screening algorithm.

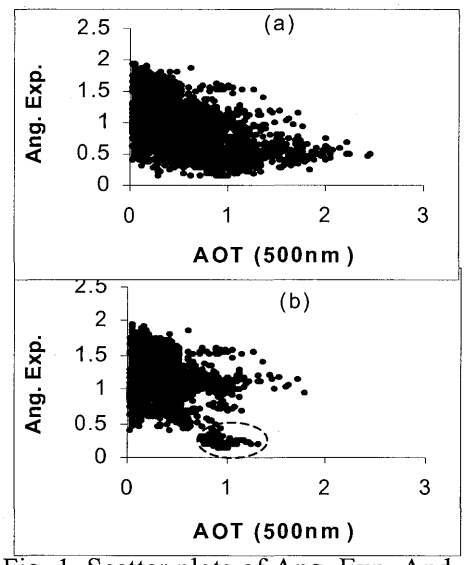

Fig. 1. Scatter plots of Ang. Exp. And AOT (500nm) (a) before cloud screening and (b) after cloud screening.

3. A study on aerosol climatology in an urban atmosphere of Chiba, Japan

a. Diurnal variations of aerosol optical properties

The results presented hereafter are for data collected in Chiba in 2006 and 2007, and are analyzed using skyrad.pack (ver. 4.2) software.[3] Figure 2 shows diurnal departures of (a) AOT (500nm), (b) Ang. Exp., and (c) SSA (500nm) from their mean values in various seasons. The diurnal variations shown in Figure 2 are related to local meteorology and/or local or foreign aerosol sources. Figure 2(a) shows that AOTs(500nm) have weak (except spring season) and strong peaks in beforenoon and afternoon periods. On that contrary, Figure 2(b) shows that Ang. Exps. have pronounced peaks in the beforenoon period than those in afternoon (except spring season) period, indicating that small and large size ranged aerosols were responsible for increasing AOTs(500nm) in the beforenoon and afternoon periods. Regardless of the season, wind speed increased in the afternoon periods, which suggested that foreign aerosols could easily transport over the observation area in the afternoon periods. SSAs (500nm) showed relatively low values (except spring season) in the beforenoon hours, which might be due to the emissions of light absorbing aerosols from automobiles in the morning hours. The interesting behavior of diurnal cycle in the spring season indicates that complex air masses influences the observation area in this season.

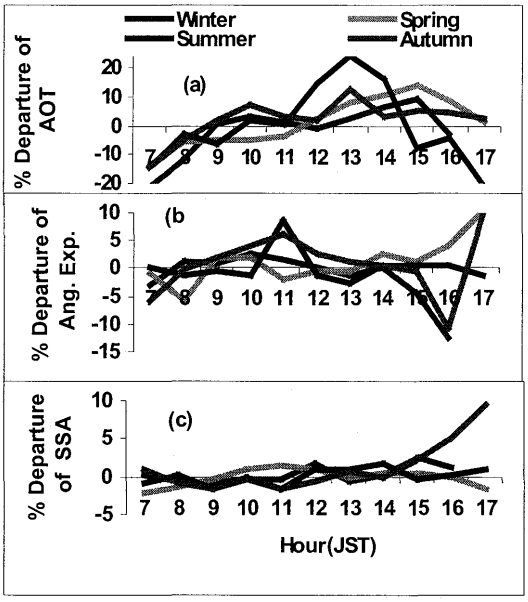

Fig. 2. Diurnal departure percentages of aerosol optical properties from their mean values at various seasons.

b. Seasonal variations of aerosol optical properties

Table 1 shows statistical analyses of aerosol optical properties for various seasons. It is understood from Table 1 that AOTs(500nm) are high in spring and summer seasons and low in winter and Autumn seasons. The moderate Ang. Exp. for the spring season indicates the mixtures of various aerosol species. Similarly, aerosols in the autumn season are observed to be strongly light absorptive in nature, wheraeas, aerosols in the spring season are comparatively more light scattering in nature. Figure 3 gives a more clear indication that aerosols in the spring season are indeed complex in nature. As observed in Figure 3, frequency distributions of AOT(500nm) and Ang. Exp. for the spring season are quite different from other seasons. Clear bimodal distribution of AOT(500nm) is evident in the spring season. Additionally, a multimodal distribution of Ang. Exp. for the same season indicates the different origins of aerosols. Further, bimodal distributions of both AOT(500nm) and Ang. Exp. in the Summer season are also interesting to be noted. Though a weak mode of AOT(500nm) with relatively high values are observed, they have Ang. Exp. higher than around 1.0, indicating that they are less likely to be natural aerosols. It is possible that excessive amount of water vapor in an atmosphere in this season increases the size of aerosols and increases AOT (500nm).

Table1. Statistical analyses of aerosol optical properties

	AOT(500nm)	Ang. Exp.	SSA(500nm)	ASY(500nm)
Win.	0.19± 0.11	1.4± 0.27	0.88± 0.08	0.68± 0.04
Spr.	0.38± 0.21	1.11± 0.41	0.93± 0.07	0.68± 0.03
Sum.	0.47± 0.28	1.31± 0.30	0.89± 0.08	0.71± 0.04
Aut.	0.23± 0.12	1.34± 0.24	0.82± 0.07	0.69± 0.04

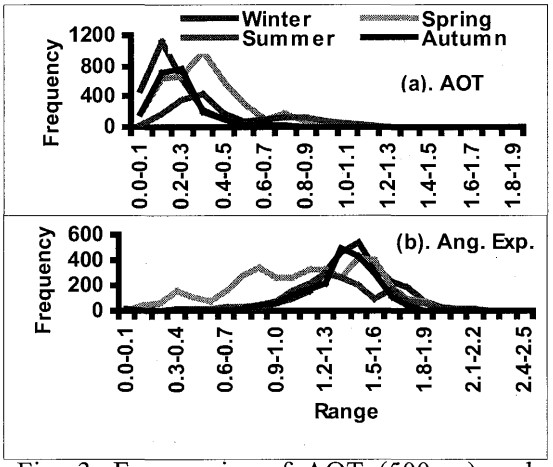

Fig. 3. Frequencies of AOT (500nm) and Angstrom Exponent on various seasons.

b. Seasonal variations of aerosol direct radiative forcing

In order to understand the effects of aerosols on atmospheric heat budget, aerosol radiative forcings at the surface and top of the atmosphere (TOA), and atmospheric radiative forcing are estimated for each season. The calculations are made using a SBDART radiative transfer model.[4] The major inputs in a radiative transfer model are spectral data of AOT, SSA, ASY, precipitable water content measured by a microwave radiometer, total ozone concentration measured by TOMS, and spectral data of reflectances measured by MODIS. The 24 hours average radiative forcings at TOA and surface were computed for clear sky observation days detected by our algorithm. Before estimating 24 hours average radiative forcings at TOA and surface, instantaneous values of downwelling global, direct, and diffuse irradiances measured by Kipp and Zonne's radiometers were compared with computed values using SBDART model. Those comparison showed satisfactory agreement. As an example, comparison of measured and computed global fluxes are shown in Fig. 5. On average, the modeled results agreed well with their measured components, however, close look of each observation datum indicates some discrepancies. This is likely due to uncertainty in either measured global irradiance or measured aerosol optical

parameters or certain assumption made during model simulation.

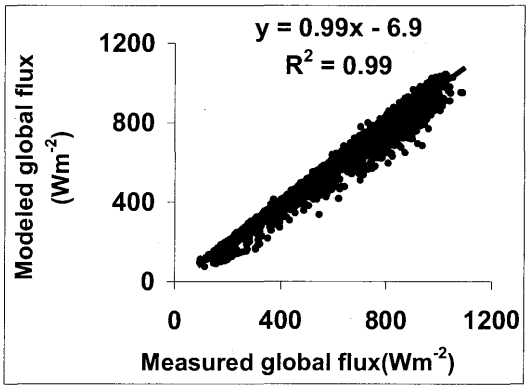

Fig. 5. A comparison between modeled and measured global irradiances.

Figures 5(a) and 5(b) show seasonal means with standard deviation of aerosol radiative forcings and aerosol radiative forcing efficiencies at the surface and TOA. The mean values of radiative forcings (radiative forcing efficiencies) in the winter, spring, summer, and autumn seasons at surface are $-12.25\pm5.21 Wm^{-2}$ ($-65.74\pm15.41 Wm^{-2}$), $-25.8\pm12.86 Wm^{-2}$ ($-71.25\pm32.9 Wm^{-2}$), $-26.53\pm15.71 Wm^{-2}$ ($-60.2\pm34.68 Wm^{-2}$) and $-15.49\pm5.05 Wm^{-2}$ ($-64.93\pm18.12 Wm^{-2}$), respectively. Similary, the respective values are $-6.95\pm3.46 Wm^{-2}$ ($-37.86\pm12.75 Wm^{-2}$), $-15.5\pm8.06 Wm^{-2}$ ($-43.22\pm22.9 Wm^{-2}$), $-11.84\pm10.98 Wm^{-2}$ ($-22.6\pm11.91 Wm^{-2}$) and $-5.81\pm4.71 Wm^{-2}$ ($-20.45\pm9.83 Wm^{-2}$) in the winter, spring, summer and autumn seasons, respectively. The radiative forcing (or radiative forcing efficiency) at TOA often reached above 0 Wm^{-2} in the autumn season for the days when SSAs(500nm) were low. The atmospheric forcing, which is a difference between radiative forcings at TOA and surface, is the highest with $14.7\pm9.5 Wm^{-2}$, whereas it is the lowest with $5.3\pm3.8 Wm^{-2}$ in the winter season. This indicated that more energy was trapped by aerosols in the summer season and less in the winter season. On the other hand, atmospheric forcing efficiency has the highest value with $44.5\pm20.5 Wm^{-2}$ in the autumn season and the lowest value with $27.9\pm16.9 Wm^{-2}$ in the winter season. This suggests that aerosols existing in the autumn season are more capable to absorb energy in the atmosphere in comparison to other seasons. Such trapped energy by aerosols is effectively used to heat the lower atmosphere.

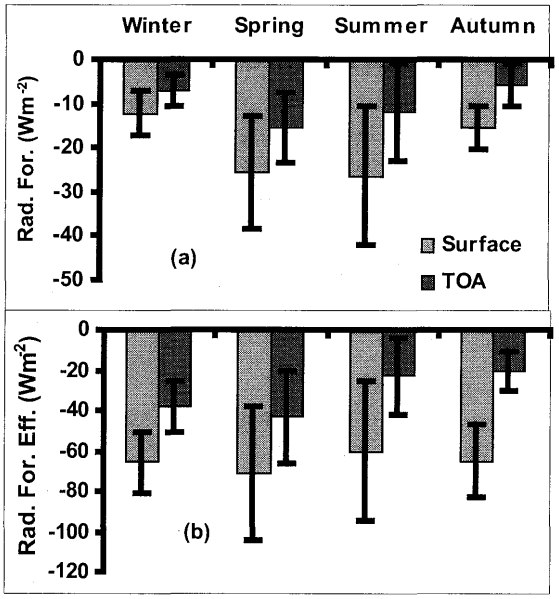

Fig. 5. Seasonal variations of (a) aerosol radiative forcing and (b) aerosol radiative forcing efficiency at top of the surface and top of the atmosphere (TOA).

Acknowledgements

This research is supported by the JSPS Fellowship Program, and also performed as a part of the SKYNET activities by the Observational Research Project for Atmospheric Change in the Troposphere (GEOSS program) of the Ministry of Education, Culture, Sports, Science and Technology, Japan.

References

1)Khatri, P. and T. Takamura, 2008:, *J. Meteor. Soc. Japan* (Submitted).

2)Kaufman, Y. J., G. P. Gobbi, and I. Koren, 2006:, *Geophys. Res. Lett.*, **33**, L07817, doi: 10.1029/2005GL025478.

3)Nakajima, T., G. Tonna, R. Rao, Y. Kaufman, and B. Holben, 1996: *Appl. Opt.*, **35**, 2672-2686.

4) Ricchiazzi, P., S. Yang, C. Gautier, and D. Sowle, 1998:, *Bull. Am. Meteorolo. Soc.*, **79**, 2101-2114.